Available online at www.sciencedirect.com
ScienceDirect
Journal of Solid State Chemistry 181 (2008) 467–472
JOURNAL OF SOLID STATE CHEMISTRY
www.elsevier.com/locate/jssc

The structure of manganese dioxide and position of proton studied by neutron diffraction with isotopic substitution

Cédric Pitteloud[b], Miki Nagao[b], Keiji Itoh[a], Ryoji Kanno[b,*]

[a]*Research Reactor Institute, Kyoto University, Kumatori-cho, Sennan-gun 590-0494, Japan*
[b]*Department of Electronic Chemistry, Interdisciplinary Graduate School of Science and Engineering, Tokyo Institute of Technology Midori-ku, Yokohama 226-8502, Japan*

Received 21 August 2007; received in revised form 1 November 2007; accepted 27 November 2007
Available online 4 December 2007

Abstract

The position of proton inside manganese dioxide, γ-MnO_2, was studied by the total neutron-scattering technique using H/D isotopic substitution. The first-order difference was obtained by subtracting the results for the two different isotopic compositions and obtaining the weighted sum of partial structure factors and radial distribution functions related to the structure around hydrogens. The deuterium-substituted γ-MnO_2 was prepared by de-intercalation of the proton via an oxidative treatment prior to re-intercalation with deuterium. The proton occupied two different positions with the H–O length of 1.0 and 1.9 Å, which corresponds to the 'Ruetschi' and 'Coleman' protons, respectively. The former protons situated in the Mn^{4+} vacant site and the latter in the tunnel centered in an oxygen octahedron. The isotopic substitution technique and the structure around protons are discussed in details.

Keywords: γ-MnO_2; Proton; Isotopic substitution; Neutron scattering

1. Introduction

Research and development in new low-cost and low-toxicity cathode materials led to the preparation of compounds such as manganese dioxides used actually in lithium or zinc primary battery [1]. Manganese oxides are present in many different forms such as α, β, γ types [2]; among them, the γ-MnO_2, and more specifically the EMD (electrolytic manganese dioxide), prepared by an electrochemical deposition from manganese sulfate aqueous solutions, exhibits the best battery performances, and many studies were carried out on the relationships between the synthesis conditions, materials characteristics and performances [3,4].

The structure of γ-MnO_2 is composed of an intergrowth of ramsdellite (R-MnO_2, space group *Pbnm*) and pyrolusite (β-MnO_2, space group $P4_2/mnm$) and can be parameterized by P_r as defined by Chabre and Pannetier [5] that represents the fraction of pyrolusite domains in a ramsdellite-based structure. The structure also contains twinning planes denoted as T_W or M_t, depending on the authors and representing the number of faults generated by twinning in the γ-MnO_2 structure. An illustration of the ramsdellite and pyrolusite with stacking faults is presented in Fig. 1. Due to highly twinned EMD produced actually, the T_W often has a value of 100 and correspond to only 50% of real twining; Guyomard [3] introduced a new model in which M_t describes the microtwining. A value of $M_t = 100$ in that case corresponds to 100% of real twining. The two models can be represented as follows: four types of stacking are possible as the succession of layers going to the right (R) direction or the left (L) direction (see Fig. 1): 'RRR' defined as $(1-\alpha)$, 'RRL' defined as α, 'LLL' defined as $(1-\beta)$ and 'LLR' defined as β. When using the T_W model ($T_W = 200 \times \alpha$ with $\alpha \leqslant 0.5$), the condition in the succession of layers used is $\alpha = (1-\beta)$. When using the M_t model ($M_t = 100 \times \alpha$ with $\alpha \leqslant 1$), the condition in the succession of layers used is $\alpha = \beta$. These two values (P_r, M_t) can be first estimated from X-ray experiments by following the positions of the (110) and (221) peaks for the P_r value; and by following the position's separation between the two

*Corresponding author. Fax: +81 45 924 5401.
E-mail address: kanno@echem.titech.ac.jp (R. Kanno).

0022-4596/$ - see front matter © 2007 Elsevier Inc. All rights reserved.
doi:10.1016/j.jssc.2007.11.030

peaks in the $54^\circ \leqslant 2\theta \leqslant 60^\circ$ region and the position of the peak around 60° (2θ) for the M_t value. Then those values can be calculated by simulation of the diffraction pattern using a program DIFFaX [6]. Those values are commonly used for comparison between different samples but are not sufficient to exactly differentiate two samples without specifying the mean redox degree of manganese as defined by the cation vacancies model [7]:

$$Mn^{4+}_{1-z-z'}Mn^{3+}_{z'}[\,]O^{2-}_{2-4z-z'}(OH^-)_{4z+z'} \quad (1)$$

can be rewritten as

$$MnO_y \cdot nH_2O \quad \text{with}$$
$$y = 2 - z'/2(1-z),$$
$$n = 2z/(1/z) + z'/2(1-z), \quad (2)$$

where [ ] denotes the cation vacancies. Our samples will then be represented by $MnO_y \cdot nH_2O$ in this study, with a set of values including P_r, M_t, y and n.

The vacancies model implied the existence of two types of protons inside the γ-MnO_2: (i) the 'Ruetschi' protons compensate the Mn^{4+} vacancies, and (ii) the 'Coleman' protons are associated with the Mn^{3+}, a schematic view is presented in Fig. 2. Experiments such as inelastic neutron-scattering studies show three different kinds of protons [8–10] but information is limited to the dynamics of these protons and no pure structural studies about those protons were made even if the manganese dioxide is largely used as a commercial cathode material. We recently indicated [11], using neutron-scattering experiment, the existence of a proton directly linked to oxygen with a 1 Å distance and highlighted the presence of another proton.

The neutron first-order difference method was used first to overcome the difficulty to analyze solutions, since the scattering is usually dominated by solvent–solvent terms except for highly concentrated solutions, in order to obtain ion solvation and complexation informations. This method was then implemented by Soper et al. [12] by including hydrogen isotope substitution directly on the solvent.

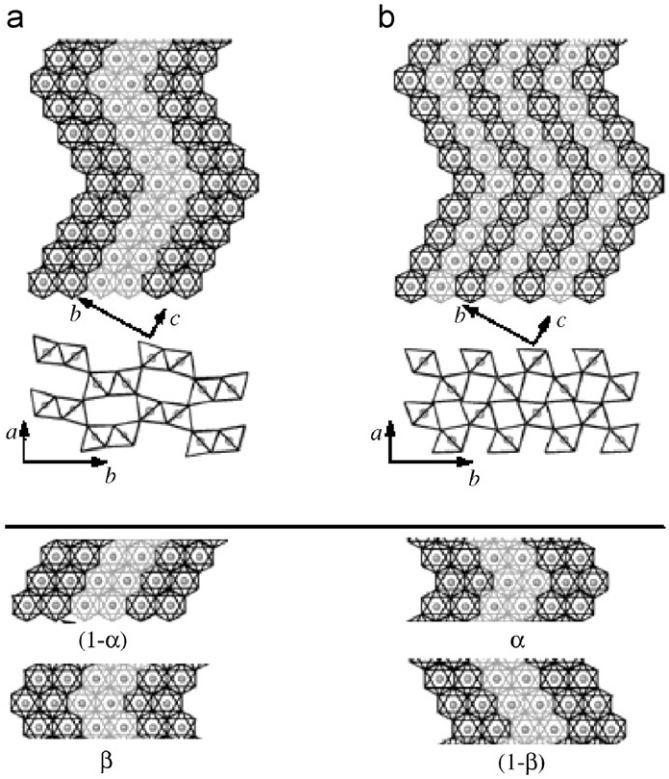

Fig. 1. Structure model of EMD for the DIFFaX calculation for (a) ramsdellite and (b) pyrolusite along the (021) basal plane of the ramsdellite. Circles correspond to Mn; dark and light symbols denote different coordinates (0 or 1/2) along the a-axis. $(1-\alpha)$, α, $(1-\beta)$ and β represent the four stackings possible for the ramsdellite (twinning).

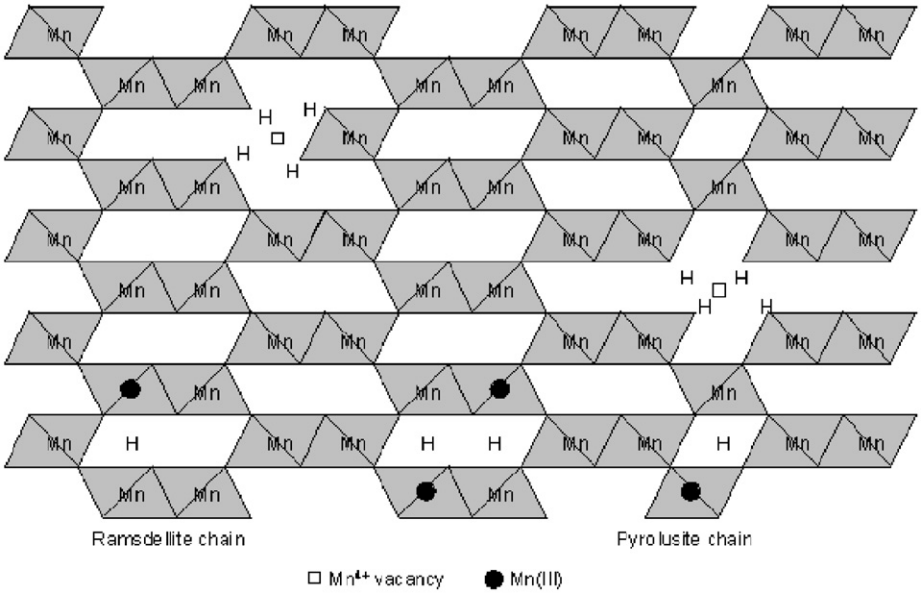

Fig. 2. Schematic view of a cation-deficient intergrowth structure of ramsdellite and pyrolusite, projection onto the (001) plane.

The technique was then successfully used for a variety of systems such as aqueous solution with alcohol [13], hydrogenated amorphous silicon [14], as a contrast tool for bio molecules [15], or to study the inter-lamellar structure of water inside clay systems [16]. All these studies led us to consider the applicability of this technique applied to the γ-MnO_2 system.

It is known that the structure of γ-MnO_2 changes during the de-intercalation of the proton by heat treatment, which happens at a relatively low temperature. This treatment is nevertheless used to prepare hydrogen-free manganese dioxide cathode for primary lithium battery. A direct exchange between H and D is not possible at room temperature and we developed a method to remove the proton without any structural change. This was achieved chemical by, using an oxidative agent. This chemical treatment can be considered as a new route to obtain hydrogen-free γ-MnO_2 with different (P_r, M_t) ratios, leading to compounds with higher effective capacity.

In this study, we have performed a series of neutron diffraction studies to extract the partial pair radial distribution function for the proton contribution to the diffraction pattern using the first-order difference method with H/D isotopic substitution. This technique offers an exact approach for separating the proton contribution and allows us to determine the precise position of the different protons inside γ-MnO_2.

2. Experimental

Electrolytic manganese dioxide (EMD, Mitsui Mining and Smelting Co., Ltd.) was used in the present study. In order to prepare the deuterium-enriched sample, the raw material was mixed with $2n$ moles of NO_2BF_4 (Aldrich, 95 + %), where n corresponds to the value obtained from $MnO_y \cdot nH_2O$, in dehydrated acetonitrile for 24 h under argon flux. After drying under vacuum, the sample was soaked in D_2O (Cambridge Isotope Laboratories, 99.96%) under magnetic agitation for 8 h prior vacuum. To avoid contamination, all manipulations involving the oxidized EMD (Oxy-EMD) or D_2O-containing samples were performed in a vacuum line or in a dry glovebox with a controlled Argon atmosphere. The composition of the EMD was determined by chemical titration and TG (thermo-gravimetric) measurements to be $MnO_{1.974} \cdot 0.286H_2O$ [7,11,17–19] (see Eqs. (1) and (2)). By a combined TG-MS (thermo-gravimetric coupled with a mass spectrometer) measurement, the isotopic purity of the sample was checked to be more than 99%.

The samples at each step, i.e before and after oxidation treatment and after the preparation of the enriched deuterium sample, were characterized by powder X-ray diffraction (XRD, Rigaku RU200B, 12 kW) and the patterns were calculated based on the model containing stacking faults using a program DIFFaX [6,19], giving the set of values (P_r, M_t) = (45, 80). No changes were observed after the oxidation or the enrichment treatment with deuterium, indicating similar pyrolusite/ramsdellite ratio and similar microtwinning amount.

Table 1
Atomic fraction calculated from the composition ($MnO_{1.974} \cdot 0.268H_2O$) and the effective densities and neutron cross sections used in the data correction procedures

	^{1}H-EMD		^{2}D-EMD
c_O		0.5899	
c_{Mn}		0.2610	
c_H or c_D		0.1491	
$\overline{M_r}$	23.90		24.05
ρ_{eff} (atom Å^{-3})	0.058		0.052
σ_s (barn)	15.29		4.20
σ_a (barn) at 1 Å	4.18		1.93

The neutron diffraction measurements were performed on the HIT-II diffractometer at the KENS pulsed spallation neutron source at KEK, Tsukuba, Japan. The samples were contained in a 4 mm i.d., 4.3 mm o.d. cylindrical titanium-zirconium cell. The diffraction patterns at ambient temperature (298 K) of the ^{1}H-hydrogen and ^{2}D-deuterium samples (H-EMD and D-EMD), the empty container, instrument background and vanadium rod were measured. The raw data were corrected for contributions due to the background, empty container, attenuation [20] and multiple scattering [21] and normalized to the scattering from the vanadium rod, giving $S(Q)$, where the modulus of the scattering vector $Q = 4\pi\sin\theta/\lambda$. The atomic densities used in the data corrections were calculated from the effective mass densities, ρ_{eff} (weight of sample divided by volume of container), and the mean atomic weights, $\overline{M_r}$, given in Table 1.

3. Results and discussion

The X-ray pattern did not show any change of the (P_r, M_t) values between H-EMD, D-EMD and Oxy-EMD samples. The oxidation treatment with NO_2BF_4, therefore, can be used to remove protons from the structure without altering it as compared with the usual heat treatment.

For the neutron-scattering experiment, the corrected, normalized intensities, $I(Q)$ are given within the static approximation [22] and for isotropic samples by

$$I(Q) = \sum_{\alpha} c_\alpha \overline{b_\alpha^2} + F(Q), \tag{3}$$

where c_α is the atomic fraction and $\overline{b_\alpha^2}$ the mean square scattering length of species α. The scattering factor, $F(Q)$, is given by

$$F(Q) = \sum_{\alpha}\sum_{\beta} c_\alpha c_\beta b_\alpha b_\beta \left[S_{\alpha\beta}(Q) - 1\right], \tag{4}$$

where b_α is the mean coherent scattering length of species α and $S_{\alpha\beta}(Q)$ are the partial structure factors. In practice, the first 'self-scattering' term in Eq. (3) is Q-dependent due to recoil effects in the scattering from light nuclei (primarily H

and D), leading to the downward slope on the $I(Q)$ with increasing Q. We therefore will denote the corrected intensities, $I^m(Q)$, to differentiate them from the true $I(Q)$ defined by Eq. (3).

If the composition of two samples are identical except for the substitution of the isotope of an element, subtracting one $I(Q)$ from the other will give, within the static approximation, the first-order difference function given by (for example using H/D substitution):

$$\Delta_H(Q) = c_H\left(\overline{b_H^2} - \overline{b_D^2}\right) + c_H^2\left(b_H^2 - b_D^2\right)[S_{HH}(Q) - 1] + \sum_{\alpha \neq H} 2c_H c_\alpha (b_H - b_D) b_\alpha [S_{\alpha H}(Q) - 1], \quad (5)$$

where H and D can be replaced by other atom isotope if other substitution is done. All partial structure factors not involving H are eliminated. The weighting factors in Eq. (5) are those given in Table 2. We can expect with H/D substitution in our EMD, elimination of the contributions related to the Mn and O interactions, concretely, elimination of the $S_{XX}(Q)$ where $X \neq$H or D in Eq. (5), leading to the partial pair radial distribution functions for the proton itself. The measured $\Delta_H(Q)$ is shown in Fig. 3. The observable residual Bragg peaks in the $\Delta_H(Q)$ indicate that the proton occupies well-defined positions in the EMD structure. Fourier transform of this corrected difference function gives the real-space information function, $G_H(r)$, given by

$$G_H(r) = \frac{1}{2\pi^2\rho_n}\int_0^\infty \left[\Delta_H(Q) - c_H\left(\overline{b_H^2} - \overline{b_D^2}\right)\right] Q^2 \frac{\sin Qr}{Qr}\, dQ = c_H^2\left(b_H^2 - b_H^2\right)[g_{HH}(r) - 1] + \sum_{\alpha \neq H} 2c_H c_\alpha (b_H - b_D) b_\alpha [g_{H\alpha}(r) - 1], \quad (6)$$

where ρ_n is the atomic number density within the EMD crystallites (i.e. independent of packing density). Based on the unit cell for pure ramsdellite and pyrolusite and on the percentage of 'De Wolff' disorder deduced from X-ray experiment, the ρ_n value of $0.127\,\text{Å}^{-3}$ was estimated. The $g_{H\alpha}(r)$ are the partial pair radial distribution functions. Fig. 4 shows the $G_H(r)$ obtained for γ-MnO_2.

The first and most intense peak centered at 0.96 Å in the $G_H(r)$ corresponds to the first O–H distance (covalently bonded hydrogen) with the standard deviation for our experiment estimated to be ± 0.01 Å. Because of the large Q-range accessible with the HIT-II instrument, no large broadening or shifting of the peak appears, allowing us to calculate coordination number via

$$n_H^O = 4\pi\rho_n c_O \int_{r_0}^{r_{min}} g_{HO}(r) r^2\, dr \approx \frac{4\pi\rho_n c_O}{2c_H c_O (b_D - b_H) b_O} \int_{r_0}^{r_{min}} [G_H(r) - G_H(0)] r^2\, dr, \quad (7)$$

where n_H^O is the mean number of oxygen atoms within a distance r_{min} of a given H-atom and $G_H(0)$ is the low r limit value of $G_H(r)$ given in Table 2. Appropriate integration of the $G_H(r)$ yields a value $n_H^O = 0.69$ for the peak around 1 Å. Here a value of 1 is expected if all the hydrogen atoms are covalently bonded to oxygen atoms. A value of $n_H^O = 0.69$ is an indication that a part of hydrogen present in our sample is not covalently bonded to oxygen. The cation vacancy had already proposed, without precise structural evidence, two kinds of proton: 'De Wolff' and 'Coleman' [19]. The 'Ruetschi' protons are associated with the Mn^{4+} vacancies in the EMD. Each empty Mn^{4+} is associated with four protons for charge compensation in the form of four OH^- ions. The 'Coleman' protons are associated with

Table 2
Weighting factors of the different $S_{H\alpha}(Q)$ and $g_{H\alpha}(r)$ in the D/H first-order difference function (see Eq. (5)) and their Fourier transform (calculated using the neutron-scattering lengths compiled by Sears [26], 1 barn = 100 fm^2)

	Weighting factor in barn	Used with
$2c_Hc_O(b_D–b_H)b_O$	10.6251	$S_{HO}(Q)$, $g_{HO}(r)$
$2c_Hc_{Mn}(b_D–b_H)b_{Mn}$	−3.0224	$S_{HMn}(Q)$, $g_{HMn}(r)$
$c_H^2(b_D^2–b_H^2)$	0.6784	$S_{HH}(Q)$, $g_{HH}(r)$
Total $= -G(0)$	8.2811	$\Delta_H(Q)$, $G_H(r)$

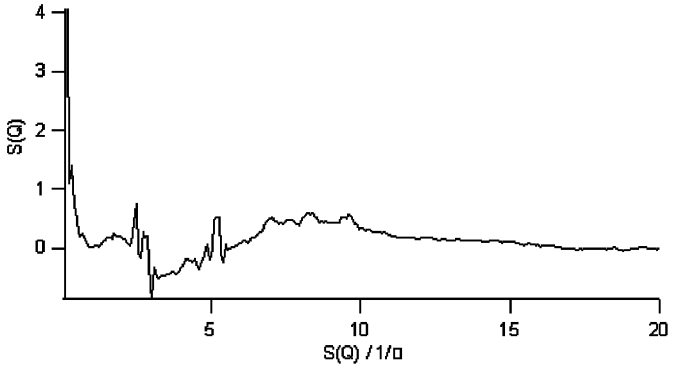

Fig. 3. The corrected interference component of the D/H first-order difference function $\Delta_H(Q)$ for γ-MnO_2.

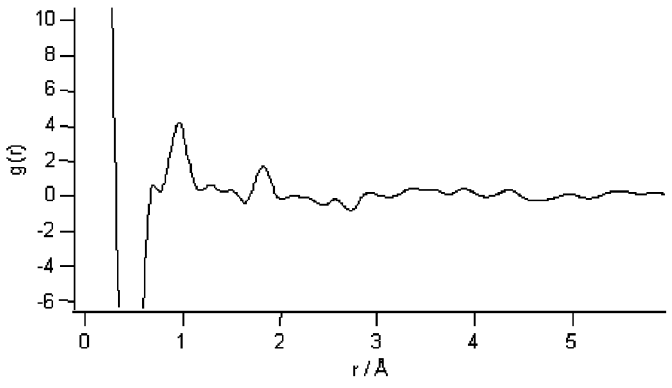

Fig. 4. The real-space first-order difference function $G_H(r)$ for γ-MnO_2 obtained by Fourier transformations of the $\Delta_H(Q)$.

Mn^{3+} cation in the tunnels of the EMD structure. By considering that only the 'Ruetschi' protons are directly bound to an oxygen (OH^- group), we can recalculate via Eq. (7) the value of c_H to satisfy a coordination number of $n_H^O = 1.0$ for the peak around 1 Å, giving a value of $c_{H1} = 0.101$ for the 'Ruetschi' proton. To satisfy the total atomic fraction of hydrogen calculated from the chemical formula, $c_H - c_{H1} = c_{H2} = 0.048$ (see Table 1), the resultant hydrogen is attributed to the 'Coleman' proton.

First principles calculations [23], for the proton close to the Mn^{4+} vacancies, located that proton between two pyramidal oxygens and they assumed an O–O distance of $2.63 < d < 2.98$ Å (or an OH–O hydrogen bond between $1.63 < d < 1.98$ Å if the O–H covalent bond is around 1 Å). Previous inelastic neutron-scattering studies indicated that the non-covalently bonded protons are delocalized and nearly free in the structure [8,10] and are centered inside an oxygen octahedron. However, Paik et al. [24] did not observe this proton. Chemical titration as described by Vetter and Jaeger [17] giving the amount of Mn^{3+} is appropriate, it gives information about the amount of possible 'Coleman' protons compensating the excess charges and is a useful tool to choose the most appropriate sample for such analysis (about 5.5% of total manganese in our sample is trivalent, Mn^{3+}).

The second peak centered with a maximum at 1.95 Å is composed by two different interactions: (i) the H-bond of the 'Ruetschi' protons with distance between $1.63 < d < 1.98$ Å as calculated by first principles calculations [23] and (ii) the 'Coleman' protons situated inside the tunnel. Integration over this peak gives $n_{H1}^O = 1$ for the 'Ruetschi' protons and $n_{H2}^O = 6.18$ for the 'Coleman' protons for the peak at 1.95 Å when using the atomic fraction c_{H1} and c_{H2}. To obtain this 6-fold coordination, the 'Coleman' proton must be centered inside the tunnel, centered inside an oxygen octahedron. The charge-compensating protons associated with an Mn^{4+} vacancy were proposed with a structure with external and internal configuration [10]. The compensating protons are situated outside the vacancies at low temperature (external) and inside the vacancies at higher temperature (internal). In the internal configuration, it was not excluded that more than one proton could be situated inside the vacancy. No peak was observed between $0.96 < d < 1.63$ Å in our neutron data, excluding the presence of two or more protons inside the same octahedron formed by oxygen. The γ-MnO_2 can be seen as an edge-sharing MnO_6 octahedron and the tunnel as an edge-sharing O_6 octahedron. We propose a configuration where the 'Ruetschi' protons situated on the common edge of two O_6 octahedrons in the 2×1 tunnel and one of the oxygen of this octahedron is also surrounding the Mn^{4+} vacancy. An example of such configuration is given as example for the 'Ruetschi'-type proton (Fig. 5a) with a hydrogen bond between $0.63 < d < 0.98$ Å, considering an O–H bond of about 1 Å. The model proposed for the 'Coleman' proton is presented in Fig. 5b.

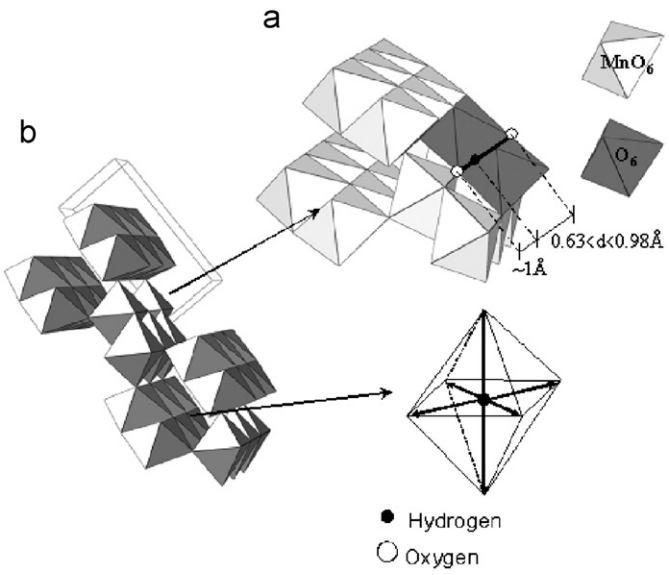

Fig. 5. Proposed model for the position of the (a) 'Ruetschi' proton close to Mn^{4+} vacancy and for the (b) 'Coleman' proton close to the Mn^{3+}.

Due to the large time scale during a neutron experiment, small fluctuations or local minimum for the positions of proton cannot be distinguished, for example the covalently bonded proton jumping rapidly from one oxygen to another one with a local minimum at the center of octahedron formed by oxygen, giving two signals in a neutron experiment. In order to assess between (a) a stable position for the 'Coleman' proton or (b) just a local position used as pathway between two 'Ruetschi' positions, experiment at low temperature is needed. In spite of that, compared to MAS-NMR or inelastic neutron scattering, the neutron-scattering experiment gives structural results, and our results must be considered as significant to assess the position of the different protons.

4. Conclusions

We have determined the position of the different protons inside the γ-MnO_2 by the neutron-scattering technique using first-order difference function with isotopic substitution. Two different positions were observed: one situated close to the Mn^{4+} vacancies with a covalent-type bond linked; and the second position lies close to the Mn^{3+} inside the tunnel of the manganese dioxide centered inside an octahedron formed by six oxygens. The NO_2BF_4 used for the oxidative treatment has an estimated $+2.1$ V redox potential in acetonitrile vs. NHE [25], and can be used to remove both kinds of proton. This treatment induced no alteration of the structure and can be proposed as a new strategy to obtain γ-MnO_2 with different ratios of 'De Wolff' and Microtwining values when compared with the usually used thermal treatment, which alters the structure.

Acknowledgments

We thank The Swiss National Science Foundation, and the Japan Society for the Promotion of Science for financial support. This work was also partly supported by a Grant-in-Aid from The Ministry of Education, Culture and Sports, Science and Technology of Japan and by Genesis Research Institute. We also thank The KEK neutron facility at Tsukuba, Japan, for neutron beam time and technical support.

References

[1] D. Glover, B. Schumm, A. Kozawa, Handbook of Manganese Dioxides-Battery Grade, T.I.B.M. Association, Cleveland, 1989.
[2] A.F. Wells, Structural Inorganic Chemistry, Oxford University Press, Oxford, 1975.
[3] S. Sarciaux, A. Le Gal La Salle, A. Verbaere, Y. Piffard, D. Guyomard, J. Power Sources 81–82 (1999) 656.
[4] S. Sarciaux, A. Le Gal La Salle, A. Verbaere, Y. Piffard, D. Guyomard, J. Power Sources 81–82 (1999) 661.
[5] Y. Chabre, J. Pannetier, Prog. Solid. State Chem. 23 (1995) 1.
[6] M.M.J. Tracey, J.M. Newsam, M.W. Deem, Computer Code DIFFaX, Vers. 1.807.
[7] P. Ruetschi, J. Electrochem. Soc. 131 (12) (1984) 2737.
[8] F. Fillaux, C.H. Cachet, H. Ouboumour, J. Tomkinson, C. Lévy-Clément, L.T. Yu, J. Electrochem. Soc. 140 (3) (1993) 585.
[9] F. Fillaux, S.M. Bennington, J. Tomkinson, L.T. Yu, Chem. Phys. 209 (1996) 111.
[10] F. Fillaux, Solid State Ionics 125 (1999) 69.
[11] M. Nagao, C. Pitteloud, T. Kamiyama, T. Otomo, K. Itoh, T. Fukunaga, R. Kanno, J. Electrochem. Soc. 152 (7) (2005) E230.
[12] A.K. Soper, G.W. Neilson, J.E. Enderby, R.A. Howe, J. Phys. C 10 (1977) 1793.
[13] J.L. Finney, A.K. Soper, J. Turner, Physical chemistry of aqueous systems: meeting the needs of industry, in: 12th International Conference on the Properties of Water and Steam, Orlando, 1995.
[14] R. Bellisent, A. Menelle, A. Chenevas-Paule, P. Chieux, J. Phys. C 8 (1985) 93.
[15] H.B. Stuhrmann, Physica B: Condens. Matter 156 (1989) 441.
[16] C. Pitteloud, D.H. Powell, H.E. Fischer, Phys. Chem. Chem. Phys. 3 (2001) 5567.
[17] K.J. Vetter, N. Jaeger, Electrochim. Acta 11 (4) (1966) 401.
[18] P. Ruetschi, J. Electrochem. Soc. 135 (11) (1988) 2657.
[19] P. Ruetschi, R. Giovanoli, J. Electrochem. Soc. 135 (11) (1988) 2663.
[20] H.H. Paalman, C.J. Pings, Appl. Phys. 33 (1962) 2635.
[21] I.A. Blech, B.L. Averbach, Phys. Rev. 137 (1965) 1113.
[22] G.L. Squires, Introduction to the Theory of Thermal Neutron Scattering, Cambridge University Press, Cambridge, 1978.
[23] D. Balachandran, D. Morgan, G. Ceder, J. Solid State Chem. 166 (1) (2002) 91.
[24] Y. Paik, W. Bowden, T. Richards, R. Sirotina, C.P. Grey, J. Electrochem. Soc. 151 (7) (2004) A998.
[25] A.R. Wizansky, P.E. Rauch, F.J. Disalvo, J. Solid State Chem. 81 (1989) 203.
[26] V.F. Sears, Neutron News 3 (3) (1992) 26.